

Pal 12 As A Part of the Sgr Stream; the Evidence From Abundance Ratios¹

Judith G. Cohen²

ABSTRACT

We present a detailed abundance analysis for 21 elements based on high dispersion, high spectral resolution Keck spectra for four members of the outer halo “young” Galactic globular cluster Pal 12. All four stars show identical abundance distributions with no credible indication of any star-to-star scatter. However, the abundance ratios of the Pal 12 stars are very peculiar. There is no detected enhancement of the α -elements; the mean of $[\text{Si}/\text{Fe}]$, $[\text{Ca}/\text{Fe}]$ and $[\text{Ti}/\text{Fe}]$ is -0.07 ± 0.05 dex, O/Fe is also Solar, while Na is very deficient. The distribution among the heavy elements shows anomalies as well. These are inconsistent with those of almost all Galactic globular clusters or of field stars in the Galaxy. The peculiarities shown by the Pal 12 stars are, however, in good general agreement with the trends established by Smecker-Hane & McWilliam and by Bonifacio *et al.* for stars in the Sgr dSph galaxy evaluated at the $[\text{Fe}/\text{H}]$ of Pal 12. This reinforces earlier suggestions that Pal 12 originally was a cluster in the Sgr dSph galaxy which during the process of accretion of this galaxy by our own was tidally stripped from the Sgr galaxy to become part of the extended Sgr stream.

Subject headings: globular clusters: general — globular clusters: individual (Pal 12) — galaxies: individual (Sgr dSph) – stars: abundances

1. Introduction

Pal 12 is a sparse globular cluster (henceforth GC) located in the outer halo of the Milky Way. The CMD studies of Gratton & Ortolani (1988) and of Stetson *et al.* (1989) suggested that Pal 12 is probably somewhat younger than the vast majority of Galactic GCs. However, until there was a measurement of the metallicity of this GC, its age could not be determined robustly due to degeneracies in the CMD between age and metallicity. Da Costa & Armandroff (1991) provided the crucial datum; they found that that Pal 12, in spite of its large galactocentric distance, is quite metal rich, obtaining $[\text{Fe}/\text{H}] = -0.6$ dex³ from low resolution spectroscopy. More recently, Brown,

¹Based in part on observations obtained at the W.M. Keck Observatory, which is operated jointly by the California Institute of Technology, the University of California, and the National Aeronautics and Space Administration.

²Palomar Observatory, Mail Stop 105-24, California Institute of Technology, Pasadena, Ca., 91125, jlc@astro.caltech.edu

³The standard nomenclature is adopted; the abundance of element X is given by $\epsilon(X) = N(X)/N(H)$ on a scale where $N(H) = 10^{12}$ H atoms. Then $[\text{X}/\text{H}] = \log_{10}[N(X)/N(H)] - \log_{10}[N(X)/N(H)]_{\odot}$, and similarly for $[\text{X}/\text{Fe}]$.

Wallerstein & Zucker (1997) carried out a high resolution spectroscopic study of two stars in Pal 12, which yielded $[\text{Fe}/\text{H}] = -1.0$ dex.

The combination of deep photometry and an estimate of $[\text{Fe}/\text{H}]$ led to the verification that Pal 12 is indeed a young cluster. Rosenberg *et al.* (1998), as part of their recent study of the age dispersion within the Galactic GC system (Rosenberg *et al.* 1999), suggest an age for Pal 12 of roughly 70% that of the majority of the halo GCs. Assuming the latter group to be 12 Gyr old, they then infer an age of 8.4 Gyr for Pal 12, consistent with that of the earlier CMD studies of Gratton & Ortolani (1988) and Stetson *et al.* (1989).

After the discovery of the Sgr dSph galaxy by Ibata, Irwin & Gilmore (1994), several groups, including Layden & Sarajedini (2000), noted that four Galactic GCs (M53, Arp 2, Terzan 7 and Terzan 8), based on their positions on the sky, appear to form a stream extending from the Sgr dSph, and suggested that these GCs had been tidally stripped away from the Sgr galaxy. The GC M54 was postulated to be the original nucleus of the Sgr galaxy.

Irwin (1999) was the first to suggest that the GC Pal 12 had also been tidally captured from the Sgr dSph galaxy by our Galaxy. Dinescu *et al.* (2000) measured the proper motion of this GC and calculated its orbit to find that Pal 12’s tidal capture from the Sgr dSph took place about 1.7 Gyr ago. Ibata *et al.* (2001) demonstrated the existence of an extended tidal stream of debris from the Sgr dSph galaxy in the Galactic halo, which has recently been detected in the 2MASS (Majewski *et al.* 2003) and in the SDSS (Ivezic *et al.* 2003) databases. Deep optical imaging over wide fields around Pal 12 by Martinez-Delgado *et al.* (2002) and by Bellazzini *et al.* (2003) show that this GC is embedded in the extended debris stream of stars torn from the Sgr dSph.

The only existing high dispersion spectroscopic study of Pal 12 (that of Brown, Wallerstein & Zucker 1997) was hitting the limits of what was observationally possible with a 4-m telescope. They analyzed the spectra of only the two brightest probable members. Their primary result was that Pal 12 did not appear to show the enhancement of the α -process elements seen in almost all GC stars. Although this is extremely interesting, the accuracy of their analysis was limited by the quality of their spectra and some key elements were not included. The purpose of the present paper is to provide a firmer foundation for their results, to extend them as possible, and to compare the properties of the Pal 12 stars with the recently published abundance distributions for stars in the Sgr dSph galaxy of Bonifacio *et al.* (2000), Smecker-Hane & McWilliam (2002) and of McWilliam, Rich & Smecker-Hane (2003).

2. Stellar Sample and Stellar Parameters

Since Pal 12 is potentially a young cluster in the outer halo, there have been, as noted above, several recent CMD studies of Pal 12. This is a rather sparse cluster, and there are only 4 probable members on the RGB brighter than $V \sim 16$ mag. These are the four stars we have observed; they are the same four stars that were observed at low resolution in the region of the IR Ca triplet

by Da Costa & Armandroff (1991). The stellar identifications we adopt are those of Harris & Canterna (1980).

As in our earlier papers, we use the V-J and V-K colors to establish the T_{eff} for these stars. We utilize the grid of predicted broad band colors and bolometric corrections of Houdashelt, Bell & Sweigart (2000) based on the MARCS stellar atmosphere code of Gustafsson *et al.* (1975). In Cohen *et al.* (2001) we demonstrated that the Kurucz and MARCS predicted colors are essentially identical, at least for the specific colors used here. The optical photometry we adopt is from Stetson *et al.* (1989) and the infrared photometry is from 2MASS (Skrutskie *et al.* 1997). The reddening is low; we adopt $E(B-V) = 0.02$ mag and a distance of 19.1 kpc from the on-line database of Harris (1996); the all-sky maps of Schlegel, Finkbeiner & Davis (1998) yield a slightly larger $E(B-V)$ of 0.036 mag. It is important to note that the distance was obtained with a knowledge of the probable young age of this anomalous GC.

The surface gravities for the Pal 12 red giants are calculated from their observed V magnitudes, their T_{eff} , the cluster distance and the reddening, as in our earlier papers. Here, however, based on the isochrones of Yi *et al.* (2002), we adopt a mass for the RGB stars of $1.0 M_{\odot}$ rather than the $0.8 M_{\odot}$ used in our earlier GC abundance analyses; the latter is appropriate for metal poor clusters with an age of 12 Gyr, but not for Pal 12.

The most luminous Pal 12 giant, star S1, is somewhat cooler than the minimum T_{eff} in the grid of Houdashelt, Bell & Sweigart (2000), and extrapolation beyond the limit of this color grid was required. The nominal T_{eff} of 3850 K so inferred from its observed colors gave poor ionization equilibrium. The photometric errors for our data produce a ± 50 K uncertainty in T_{eff} , hence we adopt a T_{eff} for this star of 3900 K. The resulting stellar parameters are listed in Table 2. The T_{eff} for the two stars analyzed by Brown, Wallerstein & Zucker (1997) (the cooler of the four stars analyzed here) are ~ 60 K higher than those adopted here; they use $V - I$ photometry in one case and a K mag for Star S1 from Cohen, Frogel & Persson (1978); the older photometry they use surely has uncertainties at least as large as that we use. Given that, the agreement in T_{eff} for the two stars in common seems reasonable.

3. Observations

All spectra were obtained with HIRES (Vogt *et al.* 1994) at the Keck Observatory. The four Pal 12 stars are too far apart on the sky to fit two within the allowed HIRES slit length, and hence each had to be observed individually. The HIRES configuration used a 1.1 arcsec wide slit (spectral resolution 34,000). Spectral coverage extended from 4650 to 7010 Å, with small gaps in coverage between the echelle orders due to the current undersized HIRES detector.

The spectra were exposed to a SNR exceeding 100 per 4 pixel resolution element in the continuum at the center of order 64 (about 5670 Å). This was calculated assuming Poisson statistics and ignoring issues of cosmic ray removal, flattening etc. These spectra were reduced using a

combination of Figaro scripts (Shortridge 1993) and the software package MAKEE⁴. Details of the exposures are given in Table 1. Heliocentric radial velocities were measured as described in Ramírez & Cohen (2002); all the stars are confirmed as members of Pal 12. The four stars have a mean heliocentric v_r of $+28.9 \text{ km s}^{-1}$, with $\sigma = 0.8 \text{ km s}^{-1}$, consistent with the presumed low mass of this cluster.

The search for absorption features present in our HIRES data and the measurement of their equivalent width (W_λ) was done automatically with a FORTRAN code, EWDET, developed for our globular cluster project. Details of this code and its features are described in Ramírez *et al.* (2001). Since we are observing only the most luminous (i.e. the coolest) stars in a high metallicity cluster, considerable hand checking of the equivalent widths had to be done at various stages of the analysis.

A list of unblended atomic lines with atomic parameters was created by merging our existing globular cluster list, developed from our earlier work on M71 and M5, adding in bluer lines in part from our work on very metal poor stars and in part as required to fill in the bluer orders covered here. We made extensive use of the NIST Atomic Spectra Database Version 2.0 (NIST Standard Reference Database #78, see (Weise *et al.* 1969; Martin *et al.* 1988; Fuhr *et al.* 1988; Weise *et al.* 1996)). The online Solar spectrum taken with the FTS at the National Solar Observatory of Wallace *et al.* (1998) and the set of Solar line identifications of Moore *et al.* (1966) were also used. The list of lines identified and measured by EWDET is then correlated, taking the radial velocity into account, to the list of suitable unblended lines to specifically identify the various atomic lines.

All lines with W_λ exceeding $200 \text{ m}\text{\AA}$ were rejected, except for the 6141.7 and 6496.9 \AA lines of Ba II. The even stronger 4934 \AA line of Ba II was eliminated; its W_λ exceeded the cutoff in all the sample stars. The list of equivalent widths used in this analysis for each of the four stars in Pal 12 is given in Table 3.

To the maximum extent possible, the the atomic data and the analysis procedures used here are identical to those developed in our earlier papers on M71 and on M5 (Cohen *et al.* 2001, Ramírez *et al.* 2001; Ramírez & Cohen 2002; Ramírez & Cohen 2003). We use HFS corrections from Prochaska *et al.* (2000) for Sc II, V I, Mn I, Co I. For Ba II, we adopt the HFS from McWilliam (1998). We use the laboratory spectroscopy of Lawler, Bonvallet & Sneden (2001) and Lawler *et al.* (2001) to calculate HFS corrections for La II and for Eu II. We have updated our Nd II gf values to those of Den Hartog *et al.* (2003).

We use the Solar abundances of Grevesse & Sauval (1998), modified for the special cases of La II, Nd II and Eu II to those found by the respective recent laboratory studies cited above. In particular, this means we have adopted $[\text{Fe}/\text{H}]$ for the Sun of -4.48 dex , although in our earlier papers on M71 and M5 we used -4.56 dex for $[\text{Fe}/\text{H}](\text{Sun})$.

⁴MAKEE was developed by T.A. Barlow specifically for reduction of Keck HIRES data. It is freely available on the world wide web at the Keck Observatory home page, <http://www2.keck.hawaii.edu:3636/>.

The microturbulent velocity (v_t) of a star can be determined spectroscopically by requiring the abundance to be independent of the strength of the lines. We apply this technique here to the large sample of detected Fe I lines in each star, and use $v_t = 1.7$ or 1.8 km s^{-1} for the four Pal 12 stars.

4. Abundance Results for Pal 12

Given the derived stellar parameters from Table 2, we determined the abundances using the equivalent widths obtained as described above. The abundance analysis is carried out using a current version of the LTE spectral synthesis program MOOG (Sneden 1973). We employ the grid of stellar atmospheres from Kurucz (1993) with a metallicity of $[\text{Fe}/\text{H}] = -1.0 \text{ dex}$ ⁵ to compute the abundances of O, Na, Mg, Si, Ca, Sc, Ti, V, Cr, Mn, Fe, Co, Ni, Cu, Zn, Y, Zr, Ba, La, Nd and Eu using the four stellar atmosphere models with the closest T_{eff} and $\log(g)$ to each star’s parameters. The abundances were interpolated using results from the closest stellar model atmospheres to the appropriate T_{eff} and $\log(g)$ for each star given in 2. The results for the abundances of these species in the four stars in Pal 12 are given in Table 4.

Table 6 of Ramírez & Cohen (2002) (which discusses M71, a GC of similar overall abundance) is a sensitivity table presenting the changes in deduced abundances of various species for small changes in T_{eff} , $\log(g)$, and v_t ; the entries in this table for the cooler stars in M71 ($T_{\text{eff}} = 4250 \text{ K}$) can be used for the Pal 12 stars as well.

The ionization equilibrium for both Fe I versus Fe II and for Ti I versus Ti II is satisfactory. The average difference for the four stars in Pal 12 between $[\text{Fe}/\text{H}]$ as inferred from Fe II lines and from Fe I lines is $+0.11 \pm 0.07 \text{ dex}$ and $+0.16 \pm 0.07 \text{ dex}$ for Ti⁶. The Fe ionization equilibrium shifts by 0.2 dex for a 100 K change in T_{eff} in this temperature regime, hence a systematic increase of the adopted T_{eff} values by 50 K would eliminate these small discrepancies. This possible systematic offset, for which no correction has been made, is slightly smaller than the uncertainty in T_{eff} . It might result from adopting a reddening for Pal 12 which is slightly too small.

No non-LTE corrections have been applied.

4.1. Comments on Individual Elements

The oxygen abundance is derived from the forbidden lines at 6300 and 6363 Å. The subtraction of the night sky emission lines at these wavelengths was reasonably straightforward. The radial

⁵We use the grid of models without convective overshoot.

⁶Due to the possible presence of random errors in stellar parameters, all abundance ratios are assigned a minimum uncertainty of 0.05 dex.

velocity of Pal 12 is sufficiently different from 0 km s⁻¹ and the stellar [O I] lines in the spectra of the Pal 12 stars are strong enough that their W_λ can be reliably measured. The C/O ratio was assumed to be Solar. The O abundance is given with respect to [Fe/H] deduced from lines of Fe I; the mean [O/Fe] becomes 0.09 dex smaller if expressed using the Fe II lines instead. The IR triplet at 7770 Å is beyond the wavelength range of these spectra. No corrections were made for the Ni I blend in the 6300 Å discussed by Allende Prieto, Lambert & Asplund (2001); when this and the small difference in adopted gf value are taken into account, their value for the Solar O abundance agrees with that adopted here to within 0.05 dex.

No lines of Al can be reached with this HIRES configuration.

There are two detected lines of Cu, both of which have very large HFS corrections, ranging between -0.5 and -1.0 dex. The abundance of copper in Pal 12 is therefore quite uncertain.

Three lines of Y II are used here. They are all crowded, and the line at 5205.4 Å is too blended to use in all but the hottest star. The gf values are from Hannaford *et al.* (1982), and give good results for the Sun. In the hottest star, the three lines gives reasonably consistent results. However, for star S1, the coolest star, the 4883.7 Å line gives an abundance more than a factor of 10 higher than the 5087.4 Å line. We are not using any HFS corrections for Y. Hannaford *et al.* (1982) suggest they are small, but perhaps the Y lines are so strong in this star that use of HFS is required. In computing the mean Y abundance for Pal 12, we ignore star S1.

4.2. Abundance Spreads

We calculate the mean abundance for each atomic species (X) with observed absorption lines for the four stars in Pal 12 as well as the 1σ rms value about that mean. These values are given in the first 3 columns of Table 5. This is compared to the observational uncertainty $[\sigma(obs)]$, given in the fourth column of the Table. $\sigma(obs)$ is taken as the uncertainty of the mean abundance for a single star, i.e. the 1σ rms value about the mean abundance of species X in a star/ \sqrt{N} , where N is the number of observed lines of species X . Values of N can be found in Table 4. This definition of the observational uncertainty presumes that errors in the W_λ and the atomic data dominate; random errors in T_{eff} or $\log(g)$ are not included. Some species, an example being Fe I with its very large value of N , have very small values of $\sigma(obs)$; we adopt a minimum of 0.05 dex for this parameter.

The ratio of these two different σ values is an indication of whether there is any intrinsic star-to-star variation in [X/Fe]. A high value of this “spread ratio” (SR), tabulated in the next to last column of this table, suggests a high probability of intrinsic scatter for the abundance of the species X .

The spectrum of the coolest Pal 12 star (S1) is the most crowded and blended and also has many lines whose W_λ exceeds the cutoff value of 200 mÅ. For three species, this reduces the number

of detected lines to only a single line in this star, while the other three Pal 12 stars in our sample have two or more detected lines. Thus in the case of Mg I, Zn I and Nd II (as well as Y II, see above), the averages and other statistics given in Table 5 are calculated using only three stars, ignoring the coolest one.

Inspection of Table 5 shows that for most species $0.6 < SR \leq 1.0$, indicating no sign of an intrinsic star-to-star range in abundance. Only for O, Cu, Zn, Zr, La and Nd does SR exceed 1.0. Copper has by far the largest calculated SR value; we believe that uncertainties associated with the large HFS corrections are responsible for the large spread in the derived Cu abundance among the four Pal 12 stars. Ignoring Cu, all the remaining species listed above have only two detected lines at best (except for Zr I, which has 3), many of the detected rare earth lines are weak, and some are crowded. We feel that when N is very small ($N < 4$), our estimate of $\sigma(obs)$ is biased low, and hence the SR is biased high. Thus there is no credible evidence from our data for an abundance spread for any species included in our analysis. In particular, the total range of $[Mg/Fe]$ is only 0.02 dex (excluding star S1, where only 1 Mg I line could be used), the total range of $[Si/Fe]$ for all four Pal 12 stars is only 0.11 dex, etc.

We have derived $[Fe/H]$ for Pal 12 which is 0.2 dex higher than that of Brown, Wallerstein & Zucker (1997), who found $[Fe/H] = -1.0 \pm 0.1$ dex. Only a small part (~ 0.05 dex) of that difference can be attributed to the cooler values of T_{eff} adopted here. We add detections for the species O I, V I and Nd II, not included in the previous work on this GC, and our abundances are much more precise than those of the previous study. We have a sample large enough to assess the possible presence of abundance spreads. To within their rather large errors, the Brown, Wallerstein & Zucker (1997) abundance ratios agree with those we have derived. They correctly discerned the general nature of Pal 12’s peculiarities.

5. Comparison of the Abundances with Those of Other Stellar Systems

In this section we compare the abundance distribution of Pal 12 with those of various other galactic populations. These patterns reflect the history of star formation, the form of the initial mass function, and the gas flows within the Galaxy. They provide signposts as to the nucleosynthesis in the early Universe and the nature of the formation and collapse of the Galaxy. Since the abundance distribution of the stars in Pal 12 is so anomalous, we seek to find analogs of it within other stellar components of the Galaxy.

5.1. Comparison with Galactic GCs

We compare the abundance ratios we have derived for Pal 12 with those of typical Galactic GCs. We adopt M71 and M5 as representative Galactic GCs of suitable metallicity; Pal 12 has $[Fe/H]$ close to that of M71. We use the data from Ramírez & Cohen (2002) for M71 and from Ramírez &

Cohen (2002) for M5; these previous analyses from our group are almost directly comparable with the present one for Pal 12 with no adjustments necessary. Figure 1 presents the abundance ratios as a function of atomic number for species between oxygen and Zr. Those of M71 and of M5 are shown in the lower panel.

There are some features in common between the M71, M5 and Pal 12 stars, particularly the large odd-even effect, which refers to the unusually large deficiency of the odd atomic number species (including Na, Al, Sc, V, Mn, and Co) compared to their even atomic number neighbors in the regime from Na to Ni in the periodic table⁷. However, there are also real and important differences. In particular, the α elements Si, Ca, and Ti as well as O, are substantially enhanced in M5 and in M71, as well as in essentially all GC stars, with $[\alpha/\text{Fe}] \sim +0.3$ dex. Pal 12, on the other hand, shows no enhancement of these elements, with the average of the mean values of $[\text{Si}/\text{Fe}]$, $[\text{Ca}/\text{Fe}]$ and $[\text{Ti}/\text{Fe}]$ being -0.07 ± 0.05 dex; $[\text{O}/\text{Fe}]$ is also almost the Solar value in Pal 12 (see Table 5). The deficiency of Na is very large in Pal 12 (the mean for the four Pal 12 stars of $[\text{Na}/\text{Fe}]$ is -0.51 ± 0.04 dex), much larger than is seen in Galactic GCs.

Figure 2 shows the heavy elements from Y to Eu. The presence of enhanced Eu in Pal 12 and in the comparison GCs M71 and M5 suggests a substantial contribution from the r -process. The $[\text{Eu}/\text{Nd}]$ and $[\text{Eu}/\text{La}]$ ratios in Pal 12 are each within 0.2 dex of that of the Solar r -process ratio determined by Burris *et al.* (2000) from the isotopic breakdowns of Käppeler, Beer & Wisshak (1989). However, Y and Zr show substantially larger deficiencies than are seen in Galactic GCs.

5.2. Comparison with Galactic Field Stars in the Halo and in the Disk

We compare the properties of Pal 12 with those of Galactic disk and halo stars. Reddy *et al.* (2003) have completed an extremely accurate and internally consistent analysis of 181 F and G dwarfs the vast majority of which belong to the Galactic thin disk. They cover the metallicity range $-0.7 \leq [\text{Fe}/\text{H}] \leq +0.2$. Their results are not consistent with the behavior of Pal 12, which is only slightly more metal poor than the metal-poor end of their sample. While the behavior of the α -elements Si, Ca and Ti agree between the disk star sample and Pal 12, the behavior of Na is highly discrepant. In the disk stars, $[\text{Na}/\text{Fe}]$ rises from Solar to about $+0.15$ dex at the metal-poor end of their sample, while that for Pal 12 is -0.51 ± 0.04 dex. The behavior of $[\text{Mn}/\text{Fe}]$ is consistent between the disk stars and Pal 12, but heavier than Fe, the agreement deteriorates again. The disk stars show $[\text{Zn}/\text{Fe}]$ rising to reach about $+0.1$ dex over this same range, while for Pal 12, $[\text{Zn}/\text{Fe}] = -0.51 \pm 0.13$ dex. Y/Fe and Eu/Fe retain their Solar ratios throughout the metallicity range covered by Reddy *et al.* (2003), while those of Pal 12 are -0.48 ± 0.12 and $+0.61 \pm 0.06$ respectively.

A detailed study of a sample of stars from the thick disk has been carried out by Prochaska

⁷The Solar abundances themselves with respect to H, $[\text{X}/\text{H}]$, show a strong odd-even effect, but what we are referring to here is an enhancement of this beyond what is characteristic of the Solar composition.

et al. (2000). These stars, which reach to lower metallicities than do the thin disk stars, also show large enhancements of the α elements, with Na and Zn also enhanced. Thus their abundance distribution also fails to match that of Pal 12.

Fulbright (2002) and Stephens (1999) have analyzed large samples of Galactic halo field stars. Fulbright (2002) attempted to correlate their kinematics with their abundance distributions. He uses the Galactic rest frame velocities (V_{RF}), calculated from the UVW velocities, removing the rotational velocity of the Local Standard of Rest, to characterize the kinematic properties of the stars in his sample. Dinescu *et al.* (2000) have measured the proper motion of Pal 12, and suggest that the apogalactic radius for its orbit is 29.4 ± 6.0 kpc. From their data we calculate $V_{RF}(\text{Pal 12})$ to be 251 ± 35 km s $^{-1}$.

Fulbright (2002) finds that the highest velocity stars in his sample have slightly lower α -enhancements than are typical of most halo stars. A similar result was obtained by Stephens & Boesgaard (2002), who concentrated on a sample of kinematically peculiar stars in the outer halo. These low α -enhancements seen in a few stars which are probably in the outer Galactic halo are not as low as those we observe in Pal 12.

The shift from the lighter to the heavier s -process elements between the first s -process (the Zr-peak) peak towards the second peak at Ba seen in Pal 12 is also not matched by the halo stars. The trends for most element ratios with increasing (V_{RF}) found among halo stars by Fulbright (2002) in general have the right sign to reproduce the behavior of Pal 12 eventually, but fail to do so by significant amounts even for his highest velocity bin, ($V_{RF} > 300$ km s $^{-1}$).

There are a very small number of metal-poor Galactic halo stars known to have unusually low abundances of α -elements, among the most extreme of which is BD +80 245, which shows near-Solar α/Fe with $[\text{Fe}/\text{H}] \sim -2$ dex (Carney *et al.* 1997). However, even these stars, a small heterogeneous group of which were studied by Ivans *et al.* (2003), fail to match the abundance ratios seen among the Pal 12 stars.

5.3. Comparison with the Sgr dSph Galaxy

As shown above, the abundance distribution within Pal 12 fails to match that of typical Galactic GCs, of most Galactic halo stars, and of Galactic disk stars. We next see how well it matches that of stars within the Sgr dSph galaxy. We utilize the results of Bonifacio *et al.* (2000), who analyzed two stars, and of Smecker-Hane & McWilliam (2002), who analyzed 14 Sgr stars. Results for $[\text{Mn}/\text{Fe}]$ from the latter sample are reported by McWilliam, Rich & Smecker-Hane (2003). Bonifacio *et al.* (2000) characterizes their results for two stars with $[\text{Fe}/\text{H}] \sim 0.2$ dex by stating “the abundance ratios found are essentially Solar with a few exceptions: Na shows a strong overdeficiency, the heavy elements Ba to Eu are overabundant, while Y is underabundant.” This is a concise approximate description of the abundance ratios in Pal 12.

We compare the mean α element ratio, $[\alpha/\text{Fe}]$, defined as the average of $[\text{Si}/\text{Fe}]$, $[\text{Ca}/\text{Fe}]$ and $[\text{Ti}/\text{Fe}]$, for stars in the Sgr dSph galaxy and for Pal 12. This is shown in the lower panel of Figure 3 as a function of metallicity. The Sgr system at low metallicity behave like typical Galactic GCs, while at high metallicity, the α -enhancement drops to zero. Pal 12 fits right on this trend. The upper panel shows the same for $[\text{Na}/\text{Fe}]$, where Pal 12 shares the tendency shown by the more metal-rich Sgr stars to show very large depletions of Na. Also shown on this figure is are the mean abundance ratios for a sample of five RGB stars in M54, a Galactic GC long believed to have been tidally stripped from the Sgr dSph galaxy, with data from Brown, Wallerstein & Gonzales (1998). Very preliminary results for three stars in Terzan 7, another Galactic GC long suspected to be stripped from the Sgr dSph galaxy, are reported by Sbordone *et al.* (2003), who find $[\text{Fe}/\text{H}] = -0.57$ dex, with Solar α/Fe , consistent with our Pal 12 result and with the run of the Sgr dSph stars.

The unusually low α -ratios seen among the more metal-rich of the Sgr dSph stars are also seen in other dwarf spheroidal galaxies. Initial spectroscopic analyses from Keck/HIRES spectra for abundances in the Draco and the U Minor dSph galaxies have been carried out by Shetrone, Bolte & Stetson (1998) and by Shetrone, Côté & Sargent (2001), with a total sample of six stars in each of these two galaxies. In both of these galaxies, the α elements (Si, Ca, Ti) appear to be less enhanced relative to Fe than they are in the Galactic halo field. The four southern dSph galaxies with small samples of stars studied with UVES (Shetrone *et al.* 2003; Tolstoy *et al.* 2003) (Sculptor, Fornax, Carina and Leo I) also show this pattern. Thus this is now a well established result for the metal-rich component of the dSph satellites of the Galaxy.

Figure 4 shows the ratios $[\text{La}/\text{Fe}]$, $[\text{La}/\text{Eu}]$ and $[\text{La}/\text{Y}]$ as a function of $[\text{Fe}/\text{H}]$ in a manner similar to that of Figure 3. Again the Sgr stars show a systematic trend of each ratio with metallicity. In each panel of this figure, both the Pal 12 point and the M54 point lie on the trend at the metallicity appropriate for the GC. The shift of the La/Eu ratio between low and high metallicity Sgr stars (with Pal 12 behaving like a low metallicity Sgr star) is equivalent to the shift between r and s -process dominance among Galactic halo stars (see, e.g. Burris *et al.* 2000).

It should be noted that a direct comparison of the Pal 12 abundance ratios with the results of Bonifacio *et al.* (2000) does not suggest very good agreement. However, the two Sgr stars studied by them both have $[\text{Fe}/\text{H}] \sim -0.25$ dex, quite different from that of Pal 12, and such a comparison must be made with Sgr stars of the appropriate metallicity.

5.4. The Age-Metallicity Relation for Sgr

Here we review the age-metallicity relation for the Sgr dSph galaxy and demonstrate that the measured metallicity and inferred age for Pal 12 are consistent with that, to within the large uncertainties. Ages for GCs can be determined through isochrone fitting or through differences between the HB and the main sequence turnoff from suitable multi-color photometry. The age of

Pal 12 has been determined by Gratton & Ortolani (1988), Stetson *et al.* (1989), and most recently by Rosenberg *et al.* (1998). Ages for the four GCs which have long been believed to be associated with the Sgr galaxy (M53, Arp 2, Terzan 7 and Terzan 8) are given by Layden & Sarajedini (2000), as are the most recent abundance determinations for these objects. Smecker-Hane & McWilliam (2002) have estimated ages for the 14 stars in their Sgr sample; these determinations for individual stars have much larger uncertainties than those for the GCs and are further compromised by the possible depth of the galaxy along the line of sight.

Figure 5 illustrates the age-metallicity (in the form of $[\alpha/\text{H}]$) relation for the Sgr dSph stars with abundance analyses by Smecker-Hane & McWilliam (2002) and for these four Galactic GCs, as well as for Pal 12. While the ages for the Sgr stars are very uncertain, the location of Pal 12 in this figure appears consistent with the age-metallicity relationship displayed by the stars in the Sgr dSph galaxy. An analysis of more Sgr stars of varying ages and metallicities is needed to better define the age-metallicity relationship of the Sgr galaxy to refine this comparison.

5.5. Comments on Nucleosynthesis

The general principles of nucleosynthesis of the elements in stars are reviewed by Wheeler, Sneden & Truran (1989) and by McWilliam (1997). Some of the trends described above are fairly easy to explain in this context. The high α -element ratios seen in Galactic GCs and halo stars are ascribed to a very old population for which there was insufficient time for type I SN to have evolved and detonated and hence contributed their nuclear processed material (consisting mainly of Fe-peak elements) to the ISM. The relevant minimum timescale for this is difficult to estimate since the evolution of close binary systems containing a white dwarf, believed to be the progenitors of Type Ia SN, must be followed in detail including mass accretion; a recent attempt to carry out this calculation by Han & Podsiadlowski (2003) gives a minimum timescale of $\sim 3 \times 10^8$ yr. The low α -ratios seen in Pal 12 must thus be ascribed a region with an star formation ongoing for a few Gyr, thus achieving full contributions from both Type I and Type II SN. Na is largely synthesized in massive stars, even more massive than those producing the bulk of the α -elements, which subsequently explode as Type II SN. The extremely large deficiency of Na seen in Pal 12 thus is probably consistent with the low α -element ratios and may not require an IMF with a deficit of very massive stars during the initial epochs of star formation.

The odd-even effect (see Figure 1) is prominent in the region of the periodic table from Na to Co. Elements with even atomic numbers in this region of the periodic table all have their most abundant stable isotope containing even numbers of both protons and neutrons. Arnett (1971) (see also Arnett 1996) discussed the odd-even effect for production of these elements through explosive nucleosynthesis. He demonstrated that the amplitude of this effect depends on the neutron excess, with larger amplitude for smaller neutron excesses which are characteristic of metal-poor material that has not been modified by H or He burning. It has long been clear that the odd-even effect is strongly enhanced among halo stars, and this effect is seen in Pal 12 as well.

While the presence of enhanced Eu requires a substantial r -process contribution in Pal 12, there may be contributions to its inventory of heavy elements from the s -process as well. The other key feature for the heavy elements in Pal 12 is the excess deficiency of Y and Zr compared to Ba and La. The s -process elements in stars with metallicities above -1.5 dex are believed to be formed mostly in AGB stars of intermediate mass. Nucleosynthesis in such conditions, reviewed by Busso, Gallino & Wasserburg (1999), with more recent calculations by Busso *et al.* (2001), is dependent on the ratio of free neutrons to seed nuclei, presumably Fe. A larger neutron-to-seed ratio will lead to increased production of the heavier s -process elements relative to the lighter ones, i.e. to those in the Ba peak versus those near Sr, which is what is seen among the Pal 12 stars. In an extreme case, this leads to s -process production of detectable amounts of lead in very low metallicity stars (see, e.g. Cohen *et al.* 2003). Thus the anomalous ratios seen among the heavy elements in Pal 12 may be symptomatic of s -process nucleosynthesis at low metallicities.

Smecker-Hane & McWilliam (2002) give a more detailed discussion of these ideas and how they apply to their sample of Sgr dSph stars spanning a wide range of metallicity, and showing peculiarities which depend on their $[\text{Fe}/\text{H}]$.

6. Summary

We present a detailed abundance analysis for 21 elements based on high dispersion, high spectral resolution Keck/HIRES spectra for four members of the outer halo “young” Galactic GC Pal 12 which has an age of ~ 8 Gyr, $\sim 30\%$ younger than almost all GCs (Rosenberg *et al.* 1998), and is known to have a rather high metallicity for a GC in the outer halo (Brown, Wallerstein & Zucker 1997). Since the discovery of the Sgr dSph galaxy, the Galactic GCs M53, Arp 2, Terzan 7 and Terzan 8 have been believed to be associated with this galaxy, which is currently being accreted by the Milky Way. Irwin (1999) recently suggested that Pal 12 is also a Galactic GC which has been tidally stripped from the Sgr galaxy.

All four stars in our sample in Pal 12 show identical abundance distributions with no credible indication of any star-to-star scatter. However, the abundance ratios of the Pal 12 stars are very peculiar. With $[\text{Fe}/\text{H}] \sim -0.8$ dex, there is no detected enhancement of the α -elements; the mean of $[\text{Si}/\text{Fe}]$, $[\text{Ca}/\text{Fe}]$ and $[\text{Ti}/\text{Fe}]$ is -0.07 ± 0.05 dex, O/Fe is also Solar, while Na is very deficient. The distribution among the heavy elements shows anomalies as well, with a shift from the first s -process peak (Y and Zr) to the second peak (Ba and La). (Eu is highly enhanced, as is typical in Galactic GCs of similar metallicity.) We show that these abundance peculiarities are not seen among other stellar populations in the Galaxy, including almost all Galactic GCs and field stars in the disk, halo and bulge of the Galaxy.

The abundance anomalies shown by the Pal 12 stars are, however, in good general agreement with the trends established by Smecker-Hane & McWilliam (2002) and Bonifacio *et al.* (2000) for stars in the Sgr dSph galaxy, when evaluated at the $[\text{Fe}/\text{H}]$ of Pal 12. It is interesting to note that

the trend of low/no α -enhancement has been found in all high metallicity stars in all the dSph satellites of the Galaxy studied to date. The abundance peculiarities exhibited by Pal 12 can in general be explained by initiating star formation in a metal poor system, and having an extended period of star formation lasting at least a few Gyr.

Our abundance analysis of a sample of four stars in Pal 12 thus reinforces earlier suggestions that this GC originally was a cluster in the Sgr dSph galaxy which during the process of accretion of this galaxy by our own was tidally stripped from the Sgr galaxy to become part of the extended Sgr stream.

This paper is for Chris Sneden, who at his review talk in Feb. 2003 at the Carnegie symposium on “The Origin and Evolution of the Elements” appealed for someone in the audience to take another look at Pal 12. The entire Keck/HIRES user communities owes a huge debt to Jerry Nelson, Gerry Smith, Steve Vogt, and many other people who have worked to make the Keck Telescope and HIRES a reality and to operate and maintain the Keck Observatory. We are grateful to the W. M. Keck Foundation for the vision to fund the construction of the W. M. Keck Observatory. The authors wish to extend special thanks to those of Hawaiian ancestry on whose sacred mountain we are privileged to be guests. Without their generous hospitality, none of the observations presented herein would have been possible. We are grateful to the National Science Foundation for partial support under grant AST-0205951 to JGC. We thank Jason Prochaska and Andy McWilliam for providing their tables of hyperfine structure in digital form, and Andy McWilliam and Tammy Smecker-Hane for providing their Sgr dSph abundances in digital form in advance of publication.

REFERENCES

- Allende Prieto, C., Lambert, D. L., & Asplund, M., 2001, ApJ, 556, L63
- Anders, E. & Grevesse, N., 1989, Geochim. Cosmochim. Acta, 53, 197
- Arnett, W. D., 1971, ApJ, 166, 153
- Arnett, D., *Supernovae and Nucleosynthesis*, Princeton U. Press, 1996, page 275
- Bellazzini, M., Ibata, R., Ferraro, R. & Testa, V., 2003, A&A (in press) (see Astro-ph/0304502)
- Bonifacio, P., Hill, V., Molar, P., Pasquini, L., Di Marcantonio, P. & Santin, P., 2000, A&A, 359, 663
- Brown, J. A., Wallerstein, G. & Zucker, D., 1997, AJ, 114, 180
- Brown, J. A., Wallerstein, G. & Gonzales, G., 1998, AJ, 118, 1245
- Burris, D. L., Pilachowski, C. A., Armandroff, T. E., Sneden, C., Cowan, J. J. & Roe, H., 2000, ApJ, 544, 302
- Busso, M., Gallino, R. & Wasserburg, G. J., 1999, ARA&A, 37, 239
- Busso, M., Gallino, R., Lambert, D. L., Travaglio, C. & Smith, V. V., 2001, ApJ, 557, 802
- Carney, B. W., Wright, J. S., Sneden, C., Laird, J. B., Aguilar, L. A. & Latham, D. W., 1997, AJ, 114, 363
- Cohen, J. G., Frogel, J. A. & Persson, S. E., 1978, ApJ, 222, 165
- Cohen, J. G., Behr, B. B., & Briley, M. M., 2001, AJ, 122, 1420
- Cohen, J. G., Christlieb, N., Qian, Y. Z., & Wasserburg, G. J., 2003, ApJ, 588, 1082
- Da Costa, G. S. & Armandroff, T. E., 1991, AJ, 101, 1329
- Den Hartog, E.A., Lawler, J.E., Sneden, C. & Cowan J.J., 2003, ApJS, 148, 543
- Dinescu, D.I., Majewski, S.R., Girard, T.M. & Cudworth, K.M., 2000, AJ, 120, 1892
- Fuhr, J. R., Martin, G. A., & Wiese, W. L., 1988, J. Phys. Chem. Ref. Data 17, Suppl. 4
- Fulbright, J. P., 2002, AJ, 123, 404
- Gratton, R. G. & Ortolani, S., 1988, A&AS, 73, 137
- Grevesse, N. & Sauval, A. J., 1998, Space Science Reviews, 85, 161
- Gustafsson, B., Bell, R.A., Eriksson, K. & Nordlund, A&A, 1975, A&A, 42, 407

- Han, Z. & Podsiadlowski, Ph., 2003, MNRAS (in press) (see Astro-ph/0309618)
- Hannaford, P., Lowe, R. M., Grevesse, N., Biemont, E., & Whaling, W., 1982, ApJ, 261, 736
- Harris, W. E., 1996, AJ, 112, 1487
- Harris, W. E. & Canterna, R., 1980, ApJ, 239, 815
- Houdashelt, M. L., Bell, R. A. & Sweigart, A. V., 2000, AJ, 119, 1448
- Ibata, R. A., Irwin, M. J. & Gilmore, G., Nature, 370, 194
- Ibata, R., Lewis, G. F., Irwin, M., Tottenj e. & Quinn, T., 2001, ApJ, 551, 294
- Irwin, M. J., 1999, in *The Stellar Content of Local Group Galaxies*, ed. P.A.Whitelock & R.D.Cannon (San Francisco: ASP), 409
- Ivans, I. I., Sneden, C., James, C. R., Preston, G. W., Fulbright, J. P., Hoffich, P. A., Carney, B. W. & Wheeler, J. C., 2003, ApJ, 592, 906
- Ivezic, Z. *et al.*, 2003, in *Milky Way Surveys: The Structure and Evolution of Our Galaxy*, ed. D. Clemens & T. Brainerd, ASP, San Francisco (see Astro-ph/0309074)
- Käppeler, F., Beer, H. & Wisshak, K., 1989, Rep. Prog. Phys., 52, 945
- Kurucz, R. L., 1993*a*, ATLAS9 Stellar Atmosphere Programs and 2 km/s Grid, (Kurucz CD-ROM No. 13)
- Lawler, J. E., Bonvallet, G. & Sneden, C., 2001, ApJ, 556, 452
- Lawler, J. E., Wickliffe, M. E., den Hartog, E. A. & Sneden, C., 2001, ApJ, 563, 1075
- Layden, A. C. & Sarajedini, A., 2000, AJ, 119, 1760
- Majewski, S. R., Skrutskie, M. F., Weinberg, M. D. & Ostheimer, J. C., 2003, AJ (in press) (see Astro-ph/0304198)
- Martin, G. A., Fuhr, J. R., & Wiese, W. L., 1988, J. Phys. Chem. Ref. Data 17, Suppl. 3
- Martinez-Delgado, Zinn, Carrera & Gallart, 2002, ApJ, 537, L19
- McWilliam, A., 1997, ARA&A, 35, 503
- McWilliam, A., 1998, AJ, 115, 1640
- McWilliam, A., Rich, R. M. & Smecker-Hane, T. A., 2003, Astro-ph/0306600
- Moore, C. E., Minnaert, M. G. J., & Houtgast, J., 1966, *The Solar Spectrum 2935 Å to 8770 Å*, National Bureau of Standards Monograph, Washington: US Government Printing Office (USGPO).

- Prochaska, J. X., Naumov, S. O., Carney, B. W., McWilliam, A., & Wolfe, A. M., 2000, *ApJ*, 120, 2513
- Ramírez, S. V., Cohen, J. G., Buss, J., & Briley, M. M., 2001, *AJ*, 122, 1429
- Ramírez, S. V. & Cohen, J. G., 2002, *AJ*, 123, 3277
- Ramírez, S. V. & Cohen, J. G., 2003, *AJ*, 125, 224
- Reddy, B. E., Tomkin, J., Lambert, D. L. & Allende-Prieto, C., 2003, *MNRAS*, 340, 304
- Rosenberg, A., Saviane, I., Piotto, G. & Held, E. V., 1998, *A&A*, 339, 61
- Rosenberg, A., Saviane, I., Pioto, G. & Aparicio, A., 1999, *AJ*, 118, 2306
- Sbordone, L., Bonifacio, P., Marconi, G. & Buonanno, R., 2003, *Astro-ph/0309120*
- Schlegel, D. J., Finkbeiner, D. P. & Davis, M., 1998, *ApJ*, 500, 525
- Shetrone, Bolte & Stetson, 1998, *AJ*, 115, 1888
- Stetrone, Côté & Sargent, 2001, *ApJ*, 548, 592
- Shetrone et al, 2003, *AJ*, 125, 684
- Shortridge K. 1993, in *Astronomical Data Analysis Software and Systems II*, A.S.P. Conf. Ser., Vol 52, eds. R.J. Hannisch, R.J.V. Brissenden, & J. Barnes, 219
- Skrutskie, M. F., Schneider, S.E., Stiening, R., Strom, S.E., Weinberg, M.D., Beichman, C., Chester, T. *et al.*, 1997, in *The Impact of Large Scale Near-IR Sky Surveys*, ed. F.Garzon *et al.* (Dordrecht: Kluwer), p. 187
- Smecker-Hane, T. A. & McWilliam, A., 2003, *ApJ* (submitted), *Astro-ph/0205411*
- Snedden, C., 1973, Ph.D. thesis, Univ. of Texas
- Stephens, A., 1999, *AJ*, 117, 1771
- Stephens, A. & Boesgaard, A. M., 2002, *AJ*, 123, 1647
- Stetson, P.B., Vandenberg, D. A., Bolte, M., Hesser, J. E. & Smith, G. H., 1989, *AJ*, 97, 1360
- Tolstoy *et al.*, 2003, *AJ*, 125, 707
- Vogt, S. E. *et al.* 1994, *SPIE*, 2198, 362
- Wallace, L., Hinkle, K. & Livingston, W.C., 1998, N.S.O. Technical Report 98-001, <http://ftp.noao.edu.fts/visatl/README>

- Weise, W. L., Smith, M. W., & Miles, B. M., 1969, Natl Stand. Ref. Data Ser., Natl Bur. Stand. (U.S.), NSRDS-NBS 22, Vol. II
- Weise, W. L., Fuhr, J. R., & Deters, T. M., 1996, J. Phys. Chem. Ref. Data Monograph No. 7
- Wheeler, J. C., Sneden, C. & Truran, J. W., 1989 ARA&A, 27, 279
- Yi, S., Demarque, P., Kim, Y.-C. , Lee, Y.-W., Ree, C. Lejeune, Th. & Barnes, S., 2001, ApJS, 136, 417

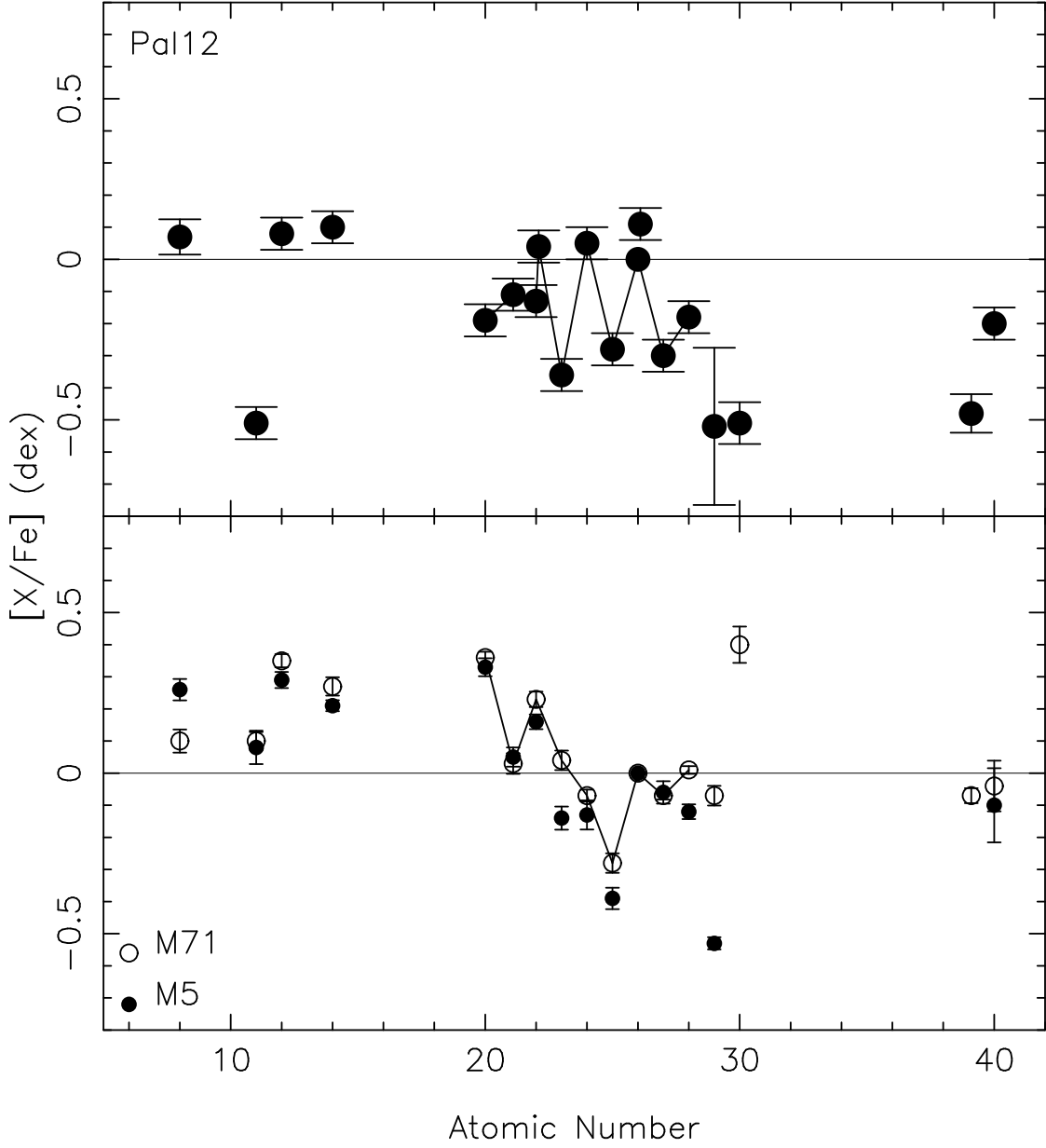


Fig. 1.— The mean abundances of the four stars in Pal 12 are shown as a function of atomic number from O through Zr in the upper panel. The same information from large samples of stars in the GCs M71 and in M5 is shown using data from Ramírez & Cohen (2002) and from Ramírez & Cohen (2002). Those points representing the abundances of species of consecutive atomic number from 20 to 28 for Pal 12 and for M71 are connected by line segments.

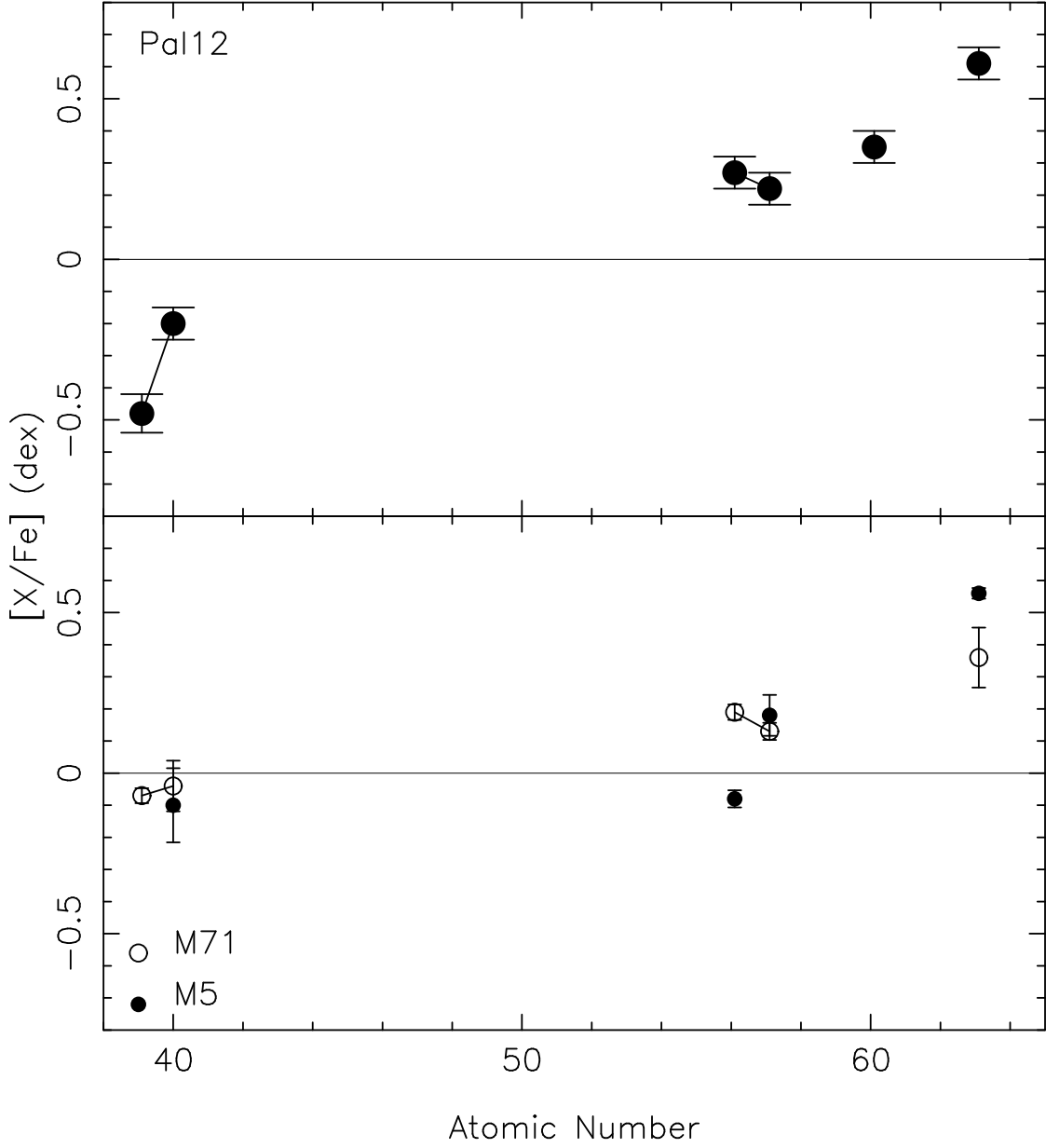


Fig. 2.— The mean abundances of the four stars in Pal 12 are shown as a function of atomic number from Y through Eu in the upper panel. The same information from large samples of stars in the GCs M71 and in M5 is shown using data from Ramírez & Cohen (2002) and from Ramírez & Cohen (2002). Those points representing the abundances of species of consecutive atomic number for Pal 12 and for M71 are connected by line segments.

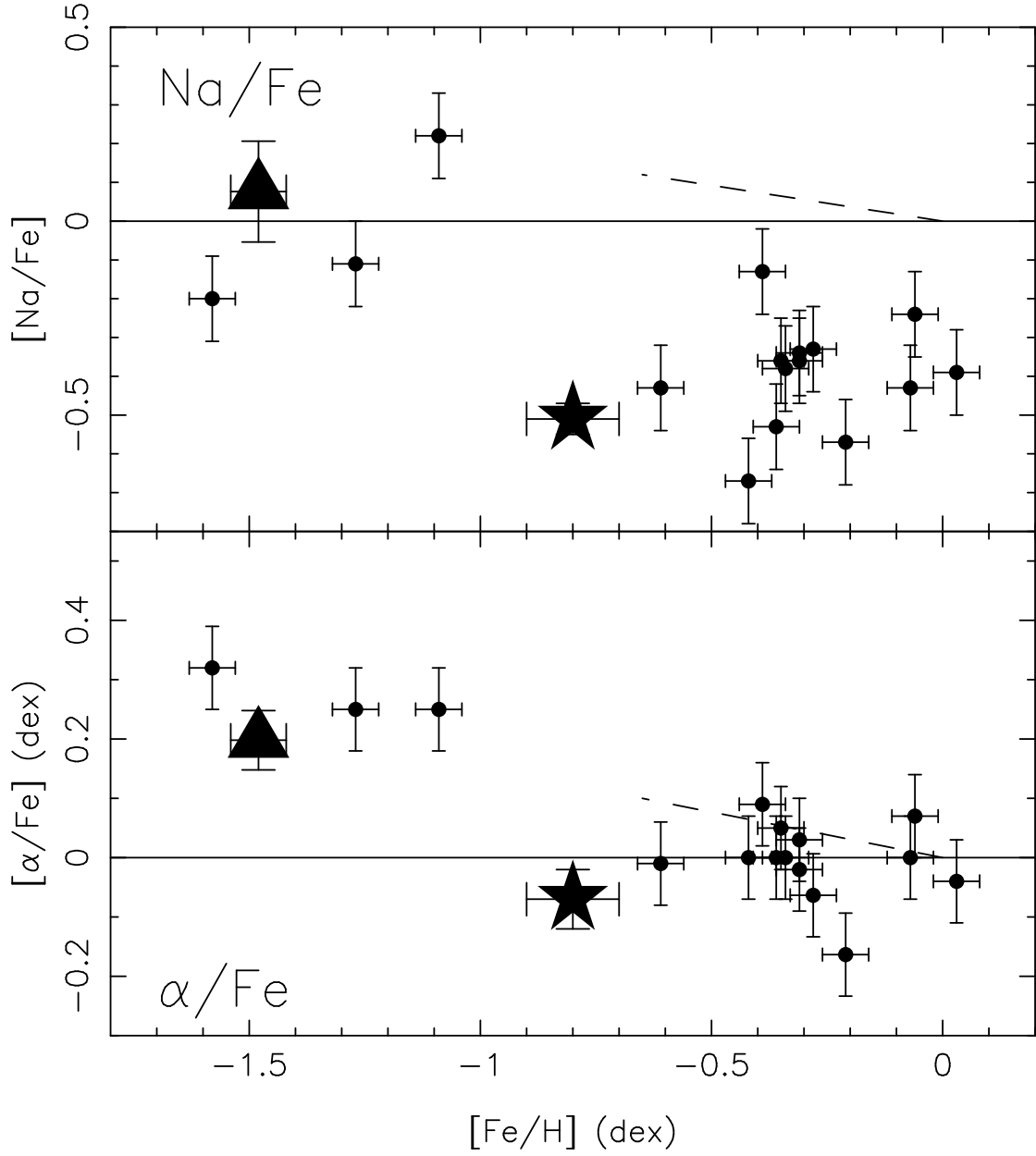


Fig. 3.— The mean abundance of the α -elements Si, Ca and Ti with respect to Fe are shown as a function of $[\text{Fe}/\text{H}]$ for a sample of stars in the Sgr dSph galaxy with data from Bonifacio *et al.* (2000) and from Smecker-Hane & McWilliam (2002). Our result for Pal 12 is indicated by the large star; that of the GC M54 is taken from Brown, Wallerstein & Gonzales (1998). The dashed line represents the behavior of the thin disk stars from Reddy *et al.* (2003). The upper panel shows the same for $[\text{Na}/\text{Fe}]$.

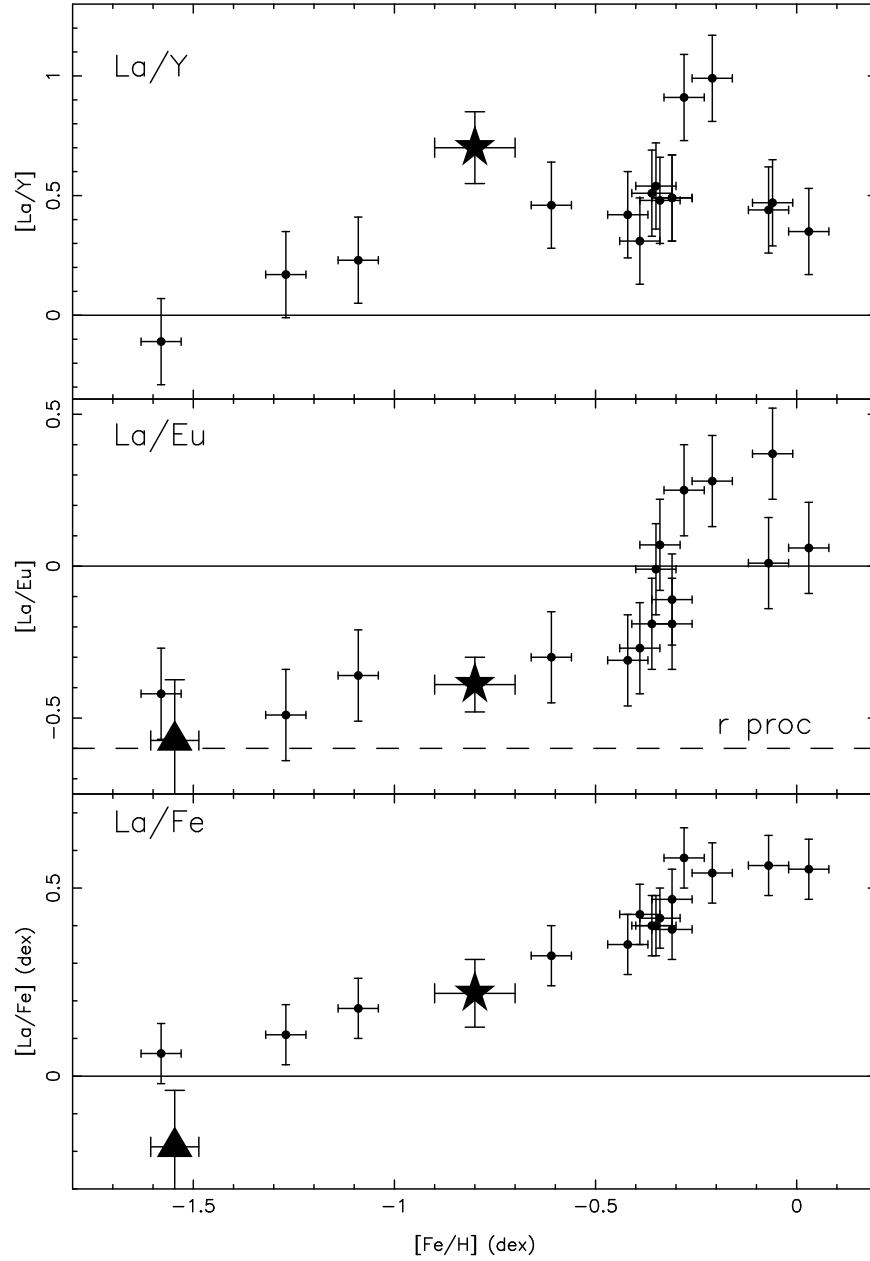


Fig. 4.— The abundance ratio $[\text{La}/\text{Fe}]$ is shown as a function of $[\text{Fe}/\text{H}]$ for a sample of stars in the Sgr dSph galaxy with data from Bonifacio *et al.* (2000) and from Smecker-Hane & McWilliam (2002) in the bottom panel. Our result for Pal 12 is indicated by the large star; that of the GC M54 is taken from Brown, Wallerstein & Gonzales (1998). The middle panel shows the same for $[\text{La}/\text{Eu}]$, while the top panel displays $[\text{La}/\text{Y}]$. The dashed line in the middle panel indicates the $[\text{La}/\text{Eu}]$ ratio from the Solar r -process.

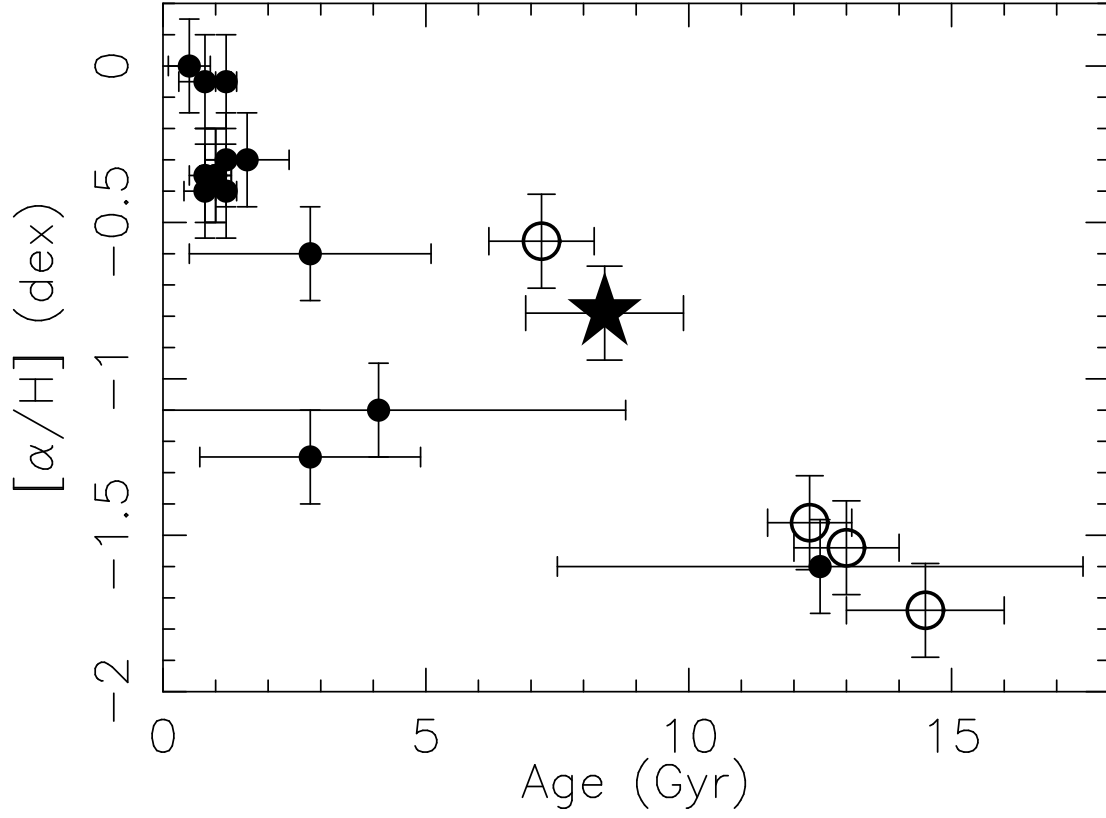


Fig. 5.— $[\alpha/H]$ versus age is shown for stars in the Sgr dSph galaxy (data from Smecker-Hane & McWilliam 2002) (small filled circles), the four Galactic GCs believed to be associated with the Sgr stream (data large from Layden & Sarajedini 2000) (large open circles), and for Pal 12 (large star).

Table 1. The Sample of Stars in Pal 12.

ID ^a	V ^b (mag)	Date Obs.	Exp. Time (sec)	SNR ^c	v_r (km s ⁻¹)
S1	14.57	6/2003	1500	> 100	+28.8
1118	14.84	6/2003	1800	> 100	+30.0
1128	15.43	6/2003	1500	> 100	+28.1
1305	15.86	8/2003	3600	> 100	+28.8

^aIdentifications are from Harris & Canterna (1980).

^bV photometry from Stetson *et al.* (1989).

^cSignal to noise ratio in the continuum near 5865 Å per 4 pixel spectral resolution element.

Table 2. Stellar Parameters for the Pal 12 Sample.

ID ^a	T_{eff} (K)	$\log(g)$ (dex)	v_t (km/s)
S1	3900	0.63	1.8
1118	4000	0.84	1.8
1128	4260	1.30	1.7
1305	4465	1.62	1.7

^aIdentifications are from Harris & Canterna (1980).

Table 3. Equivalent Widths For the Pal 12 Stars

Ion	λ (\AA)	χ (eV)	$\log gf$	$W_\lambda(\text{S1})$ (m \AA)	$W_\lambda(1118)$ (m \AA)	$W_\lambda(1128)$ (m \AA)	$W_\lambda(1305)$ (m \AA)
OI	6300.30	0.00	−9.78	68	79	39	39
OI	6363.78	0.02	−10.30	45	40	14	18
NaI	5682.63	2.10	−0.70	113	103	77	67
NaI	5688.19	2.10	−0.42	128	108	100	94
NaI	6154.23	2.10	−1.53	41	35	19	15
NaI	6160.75	2.00	−1.23	65	53	30	28
MgI	4703.00	4.34	−0.67	...	184	191	185
MgI	5528.40	4.34	−0.48	199
MgI	5711.09	4.34	−1.67	119	129	111	102
SiI	5665.55	4.92	−2.04	43	40	54	44
SiI	5690.43	4.93	−1.87	40	36	38	44
SiI	5701.10	4.93	−2.05	45	42	39	42
SiI	5772.15	5.08	−1.75	30	32	47	51
SiI	5793.07	4.93	−2.06	37	27	32	34
SiI	5948.54	5.08	−1.23	69	78	75	80
SiI	6145.02	5.61	−1.44	17	18	24	25
SiI	6155.13	5.62	−0.76	61	65	55	62
SiI	6237.32	5.62	−1.01	33	31	38	42
SiI	6721.84	5.86	−0.94	...	22	16	22
SiI	7003.57	5.96	−0.83	19	18	34	30
SiI	7005.89	5.98	−0.73	37	28	46	36
SiI	7034.90	5.87	−0.88	33	21	34	49
CaI	5512.99	2.93	−0.27	119	115	97	95
CaI	5581.96	2.52	−0.47	154	143	126	114
CaI	5588.75	2.52	0.44	...	193	174	163
CaI	5590.11	2.52	−0.71	154	143	120	111
CaI	5601.28	2.52	−0.44	177	163	140	125
CaI	6156.02	2.52	−2.19	47	42	30	14
CaI	6161.30	2.52	−1.03	154	136	108	90
CaI	6166.44	2.52	−1.05	142	121	107	88
CaI	6169.04	2.52	−0.54	158	143	124	111
CaI	6169.56	2.52	−0.27	175	162	142	127

Table 3—Continued

Ion	λ (\AA)	χ (eV)	$\log gf$	$W_\lambda(\text{S1})$ (m \AA)	$W_\lambda(1118)$ (m \AA)	$W_\lambda(1128)$ (m \AA)	$W_\lambda(1305)$ (m \AA)
CaI	6471.66	2.52	−0.59	155	140	126	119
CaI	6493.78	2.52	0.14	180	164	156	147
CaI	6499.65	2.54	−0.59	153	148	122	111
CaI	6508.85	2.52	−2.12	48	32	16	12
ScII	5526.79	1.77	0.13	114	111	102	104
ScII	5657.90	1.51	−0.50	113	120	106	103
ScII	5667.15	1.50	−1.24	80	84	62	61
ScII	5669.04	1.50	−1.12	81	87
ScII	5684.20	1.51	−1.08	79	76	71	64
ScII	6245.64	1.51	−1.13	86	78	70	74
ScII	6604.60	1.36	−1.48	91	76	71	63
TiI	4681.92	0.85	−1.07	195	...
TiI	4981.74	0.85	0.50	187	170
TiI	5022.87	0.83	−0.43	...	199	153	131
TiI	5039.96	0.02	−1.13	187	145
TiI	5426.26	0.02	−3.01	160	143	82	55
TiI	5471.20	1.44	−1.39	91	69	44	26
TiI	5474.21	1.46	−1.23	134	96	61	42
TiI	5490.15	1.46	−0.93	135	121	77	60
TiI	5648.57	2.49	−0.25	57	45	24	16
TiI	5662.16	2.32	−0.11	117	102	72	53
TiI	5689.49	2.30	−0.47	73	63	41	28
TiI	5702.69	2.29	−0.57	70	56	38	21
TiI	5739.46	2.25	−0.60	56	39	20	19
TiI	5739.98	2.24	−0.67	49	39	18	17
TiI	5866.45	1.07	−0.84	195	167	129	98
TiI	5880.27	1.05	−2.05	120	104	55	39
TiI	5922.11	1.05	−1.47	154	126	90	64
TiI	5937.81	1.07	−1.89	114	93	55	38
TiI	5941.75	1.05	−1.52	152	134	93	82
TiI	5953.16	1.89	−0.33	137	126	92	71
TiI	5965.83	1.88	−0.41	143	121	88	78

Table 3—Continued

Ion	λ (\AA)	χ (eV)	$\log gf$	$W_\lambda(\text{S1})$ ($\text{m}\text{\AA}$)	$W_\lambda(1118)$ ($\text{m}\text{\AA}$)	$W_\lambda(1128)$ ($\text{m}\text{\AA}$)	$W_\lambda(1305)$ ($\text{m}\text{\AA}$)
TiI	5978.54	1.87	−0.50	121	109	81	66
TiI	6064.63	1.05	−1.94	119	98	64	37
TiI	6091.17	2.27	−0.42	87	75	54	32
TiI	6092.80	1.07	−1.38	66	39	27	...
TiI	6126.22	1.07	−1.42	158	135	98	74
TiI	6258.10	1.44	−0.35	...	177	126	103
TiI	6258.71	1.46	−0.24	186	134
TiI	6261.10	1.43	−0.48	144	98
TiI	6303.76	1.44	−1.57	107	92	54	28
TiI	6312.22	1.46	−1.55	96	82	48	34
TiI	6743.12	0.90	−1.63	168	144	99	73
TiII	6861.45	1.24	−0.74	64	54	18	...
TiII	4657.20	1.24	−2.32	108	...
TiII	4708.67	1.24	−2.37	112	100	103	97
TiII	4865.62	1.12	−2.81	88	103	91	91
TiII	4911.20	3.12	−0.34	88	76	68	77
TiII	5185.91	1.89	−1.46	...	110	113	107
TiII	5336.79	1.58	−1.63	126	117	113	122
VI	5670.85	1.08	−0.43	156	137	94	55
VI	5703.57	1.05	−0.21	154	133	94	76
VI	6081.44	1.05	−0.58	141	119	82	46
VI	6090.22	1.08	−0.06	159	138	105	74
VI	6199.20	0.29	−1.28	...	175	108	59
VI	6243.10	0.30	−0.98	140	90
VI	6251.82	0.29	−1.34	185	158	106	65
VI	6274.64	0.27	−1.67	151	131	76	46
VI	6285.14	0.28	−1.51	158	132	84	56
VI	6504.16	1.18	−1.23	76	59	43	19
CrI	4652.17	1.00	−1.03	166	168
CrI	5345.81	1.00	−0.97	199	174
CrI	5348.33	1.00	−1.29	170	166
CrI	5783.09	3.32	−0.50	101	60	50	37

Table 3—Continued

Ion	λ (\AA)	χ (eV)	$\log gf$	$W_\lambda(\text{S1})$ (m \AA)	$W_\lambda(1118)$ (m \AA)	$W_\lambda(1128)$ (m \AA)	$W_\lambda(1305)$ (m \AA)
CrI	5783.89	3.32	−0.29	107	96	77	71
CrI	5785.02	3.32	−0.38	45	68
CrI	5787.96	3.32	−0.08	93	79	71	59
CrI	5844.59	3.01	−1.76	37	35	21	13
CrI	6978.49	3.46	0.14	121	115	91	71
CrI	6979.80	3.46	−0.41	75	64	50	39
MnI	4754.04	2.28	−0.09	199	192	163	151
MnI	4783.42	2.30	0.04	172	174
MnI	4823.50	2.32	0.14	150
MnI	5537.74	2.19	−2.02	92	54
MnI	6021.80	3.08	0.03	156	149	127	114
FeI	4788.77	3.24	−1.81	92	90
FeI	5083.34	0.96	−2.96	182	183
FeI	5198.72	2.22	−2.14	...	196	158	154
FeI	5393.18	3.24	−0.72	...	188	170	165
FeI	5406.78	4.37	−1.62	61	64	58	54
FeI	5410.92	4.47	0.40	147	153	134	134
FeI	5415.21	4.39	0.64	169	165	149	146
FeI	5417.04	4.41	−1.58	49	48	56	46
FeI	5424.08	4.32	0.51	186	178	169	160
FeI	5441.33	4.10	−1.63	49	44	51	41
FeI	5445.05	4.39	−0.03	138	126	120	116
FeI	5466.39	4.37	−0.62	112	108	97	93
FeI	5470.09	4.44	−1.71	43	32	29	27
FeI	5473.90	4.15	−0.69	104	98	97	96
FeI	5487.14	4.41	−1.43	...	78	64	55
FeI	5493.50	4.10	−1.68	82	68
FeI	5494.46	4.07	−1.99	72	50	48	41
FeI	5522.45	4.21	−1.45	68	70	59	57
FeI	5525.55	4.23	−1.08	77	87	71	78
FeI	5536.58	2.83	−3.71	34	21
FeI	5554.88	4.55	−0.35	104	109	102	101

Table 3—Continued

Ion	λ (\AA)	χ (eV)	$\log gf$	$W_\lambda(\text{S1})$ ($\text{m}\text{\AA}$)	$W_\lambda(1118)$ ($\text{m}\text{\AA}$)	$W_\lambda(1128)$ ($\text{m}\text{\AA}$)	$W_\lambda(1305)$ ($\text{m}\text{\AA}$)
FeI	5560.21	4.43	−1.10	60	64	53	53
FeI	5567.39	2.61	−2.67	145	143	129	119
FeI	5569.62	3.42	−0.49	180	177	160	159
FeI	5576.09	3.43	−0.92	162	157	144	135
FeI	5586.76	3.37	−0.14	192
FeI	5618.63	4.21	−1.63	78	74	68	66
FeI	5619.59	4.39	−1.53	50	36
FeI	5624.04	4.26	−1.22	69	...
FeI	5641.44	4.26	−1.08	95	105	90	87
FeI	5650.02	5.10	−0.82	38	42	27	36
FeI	5650.70	5.08	−0.96	31	33	31	29
FeI	5652.32	4.26	−1.85	41	37	39	33
FeI	5653.89	4.39	−1.54	58	60	49	48
FeI	5661.35	4.28	−1.76	58	56	36	37
FeI	5662.52	4.18	−0.57	140	142	117	112
FeI	5679.02	4.65	−0.82	71	73	64	66
FeI	5680.24	4.19	−2.48	34	57	23	19
FeI	5698.02	3.64	−2.58	59	48	42	37
FeI	5701.54	2.56	−2.14	172	159	141	130
FeI	5705.47	4.30	−1.36	58	63	57	50
FeI	5731.76	4.26	−1.20	85	82	73	68
FeI	5741.85	4.26	−1.85	63	57	49	42
FeI	5752.04	4.55	−0.94	76	77	77	64
FeI	5753.12	4.26	−0.69	113	115	102	97
FeI	5760.35	3.64	−2.39	60	73	55	39
FeI	5762.99	4.21	−0.41	149	146	140	129
FeI	5775.06	4.22	−1.30	85	80	72	75
FeI	5778.46	2.59	−3.43	89	85	69	67
FeI	5793.91	4.22	−1.60	55	51	47	52
FeI	5827.88	3.28	−3.31	45	36	29	20
FeI	5838.37	3.94	−2.24	43	41	28	34
FeI	5852.22	4.55	−1.23	...	86	70	54

Table 3—Continued

Ion	λ (\AA)	χ (eV)	$\log gf$	$W_\lambda(\text{S1})$ (m \AA)	$W_\lambda(1118)$ (m \AA)	$W_\lambda(1128)$ (m \AA)	$W_\lambda(1305)$ (m \AA)
FeI	5855.09	4.61	−1.48	40	44	33	23
FeI	5856.08	4.29	−1.33	82	76	56	50
FeI	5859.60	4.55	−0.55	98	98	91	80
FeI	5883.81	3.96	−1.26	108	94	92	79
FeI	5927.79	4.65	−0.99	50	51	47	49
FeI	5929.67	4.55	−1.31	53	47	47	41
FeI	5930.17	4.65	−0.14	97	91	90	92
FeI	5934.65	3.93	−1.07	134	125	107	104
FeI	5940.99	4.18	−2.05	54	52	48	38
FeI	5952.72	3.98	−1.34	100	101	91	80
FeI	5956.69	0.86	−4.50	...	182	151	124
FeI	5976.79	3.94	−1.33	106	102	96	91
FeI	5983.69	4.55	−0.66	106	98	90	91
FeI	5984.83	4.73	−0.26	109	97
FeI	6024.05	4.55	0.03	120	118	119	114
FeI	6027.05	4.07	−1.09	95	97	85	80
FeI	6055.99	4.73	−0.37	86	86	81	80
FeI	6065.48	2.61	−1.41	179	166
FeI	6078.50	4.79	−0.33	90	83	86	78
FeI	6079.00	4.65	−1.02	65	59	57	48
FeI	6089.57	5.02	−0.90	...	63	58	55
FeI	6093.67	4.65	−1.40	47	45	45	...
FeI	6094.37	4.65	−1.84	28	27	35	19
FeI	6096.66	3.98	−1.83	68	62	63	57
FeI	6137.69	2.59	−1.35	195
FeI	6151.62	2.18	−3.37	142	137	114	101
FeI	6157.73	4.07	−1.16	111	113	102	93
FeI	6165.36	4.14	−1.47	81	69	64	58
FeI	6173.34	2.22	−2.88	170	149	131	125
FeI	6180.20	2.73	−2.65	134	126	104	99
FeI	6187.99	3.94	−1.62	84	89	72	68
FeI	6200.31	2.61	−2.37	144	148	129	118

Table 3—Continued

Ion	λ (\AA)	χ (eV)	$\log gf$	$W_\lambda(\text{S1})$ ($\text{m}\text{\AA}$)	$W_\lambda(1118)$ ($\text{m}\text{\AA}$)	$W_\lambda(1128)$ ($\text{m}\text{\AA}$)	$W_\lambda(1305)$ ($\text{m}\text{\AA}$)
FeI	6240.65	2.22	−3.17	142	132	108	100
FeI	6246.32	3.60	−0.88	150	145	136	136
FeI	6252.55	2.40	−1.77	194	176
FeI	6254.26	2.28	−2.43	192	178	169	155
FeI	6265.13	2.18	−2.54	195	190	160	145
FeI	6271.28	3.33	−2.70	70	71	58	44
FeI	6290.97	4.73	−0.73	77	81	77	71
FeI	6297.79	2.22	−2.64	175	167	130	137
FeI	6301.51	3.65	−0.72	154	155	139	144
FeI	6302.50	3.69	−1.11	146	142	131	105
FeI	6311.50	2.83	−3.14	101	99	72	58
FeI	6380.75	4.19	−1.38	86	87	78	73
FeI	6392.54	2.28	−3.99	93	85	64	58
FeI	6393.60	2.43	−1.58	186
FeI	6408.03	3.69	−1.02	141	132	128	118
FeI	6411.65	3.65	−0.72	161	154	142	140
FeI	6421.35	2.28	−2.01	188	175
FeI	6469.21	4.83	−0.73	100	98	81	76
FeI	6475.63	2.56	−2.94	135	125	112	89
FeI	6481.87	2.28	−3.01	156	139	128	113
FeI	6483.94	1.48	−5.34	61	46	41	23
FeI	6495.74	4.83	−0.84	61	64	56	41
FeI	6498.94	0.96	−4.69	196	188	153	123
FeI	6533.93	4.56	−1.36	53	62	56	49
FeI	6581.21	1.48	−4.68	148	100	83	71
FeI	6592.91	2.73	−1.47	198	171	160	158
FeI	6593.87	2.43	−2.37	178	142	134	128
FeI	6608.02	2.28	−3.93	103	88	66	51
FeI	6609.11	2.56	−2.66	155	148	118	115
FeI	6625.02	1.01	−5.37	...	177	118	83
FeI	6627.54	4.79	−1.58	47	36	46	...
FeI	6633.75	4.79	−0.80	...	87	86	82

Table 3—Continued

Ion	λ (\AA)	χ (eV)	$\log gf$	$W_\lambda(\text{S1})$ ($\text{m}\text{\AA}$)	$W_\lambda(1118)$ ($\text{m}\text{\AA}$)	$W_\lambda(1128)$ ($\text{m}\text{\AA}$)	$W_\lambda(1305)$ ($\text{m}\text{\AA}$)
FeI	6646.93	2.61	−3.96	65	65	50	41
FeI	6648.12	1.01	−5.92	103	91	69	48
FeI	6713.77	4.79	−1.50	25	35	30	20
FeI	6715.38	4.61	−1.54	44	44	39	29
FeI	6716.22	4.58	−1.85	31	35	28	18
FeI	6725.35	4.19	−2.25	42	39	34	28
FeI	6726.67	4.61	−1.07	58	62	58	53
FeI	6733.15	4.64	−1.48	33	40	37	36
FeI	6739.52	1.56	−4.79	103	96	74	54
FeI	6750.15	2.42	−2.58	172	158	143	133
FeI	6752.71	4.64	−1.20	72	52
FeI	6783.71	2.59	−3.92	71	70	53	27
FeI	6786.86	4.19	−1.97	37	65	48	32
FeI	6837.02	4.59	−1.69	28	26	24	25
FeI	6839.83	2.56	−3.35	105	100	83	74
FeI	6842.68	4.64	−1.22	58	53	53	45
FeI	6843.65	4.55	−0.83	79	68	70	71
FeI	6851.63	1.61	−5.28	70	71	41	27
FeI	6855.18	4.56	−0.74	100	96	98	88
FeI	6855.71	4.61	−1.78	36	35
FeI	6858.15	4.61	−0.93	68	67	68	63
FeI	6861.95	2.42	−3.85	93	80	71	56
FeI	6862.49	4.56	−1.47	41	37
FeI	6971.93	3.02	−3.34	59	51	39	32
FeI	6978.85	2.48	−2.45	150	138
FeI	6988.52	2.40	−3.56	116	110	96	81
FeI	6999.88	4.10	−1.46	82	89	70	74
FeI	7000.62	4.14	−2.39	37	35	39	27
FeI	7014.98	4.19	−4.20	69	50	57	...
FeI	7022.95	4.19	−1.15	98	86	85	87
FeI	7038.22	4.22	−1.20	97	102	83	80
FeII	4923.93	3.23	−1.32	168	173	177	...

Table 3—Continued

Ion	λ (\AA)	χ (eV)	$\log gf$	$W_\lambda(\text{S1})$ ($\text{m}\text{\AA}$)	$W_\lambda(1118)$ ($\text{m}\text{\AA}$)	$W_\lambda(1128)$ ($\text{m}\text{\AA}$)	$W_\lambda(1305)$ ($\text{m}\text{\AA}$)
FeII	5197.58	3.22	−2.23	88	133
FeII	5234.63	3.22	−2.22	89	83	85	102
FeII	5414.08	3.22	−3.62	21	38	44	43
FeII	5534.85	3.25	−2.64	98	89
FeII	6084.11	3.20	−3.80	19	38	40	30
FeII	6149.26	3.89	−2.69	38	34	36	51
FeII	6247.56	3.89	−2.36	43	42	58	69
FeII	6369.46	2.89	−4.20	23	27	26	34
FeII	6416.92	3.89	−2.69	36	42	46	47
CoI	6516.08	1.71	−3.45	61	43	74	...
CoI	5530.79	1.71	−2.06	92	81	57	51
CoI	5647.23	2.28	−1.56	58	51	35	25
CoI	6189.00	1.71	−2.45	89	91	55	42
CoI	6632.45	2.28	−2.00	58	46	37	27
NiI	5578.72	1.68	−2.64	148	131	116	100
NiI	5587.86	1.93	−2.14	155	134	108	101
NiI	5589.36	3.90	−1.14	38	32	30	22
NiI	5593.74	3.90	−0.84	47	48	43	42
NiI	5682.20	4.10	−0.47	61	64	44	49
NiI	5748.35	1.68	−3.26	112	106	84	67
NiI	5796.09	1.95	−3.69	51	43	36	27
NiI	5805.22	1.68	−0.64	37	...
NiI	5846.99	1.68	−3.21	105	98	87	56
NiI	6053.69	4.23	−1.07	28	23	26	14
NiI	6128.97	1.68	−3.33	99	93	72	62
NiI	6175.37	4.09	−0.54	57	54	46	47
NiI	6176.81	4.09	−0.53	72	68	64	66
NiI	6177.24	1.83	−3.51	76	63	50	35
NiI	6314.66	3.54	−1.77	...	136	115	...
NiI	6370.35	3.54	−1.94	22	21	19	16
NiI	6378.25	4.15	−0.90	39	36	33	30
NiI	6482.80	1.93	−2.63	114	101	90	82

Table 3—Continued

Ion	λ (\AA)	χ (eV)	$\log gf$	$W_\lambda(\text{S1})$ (m \AA)	$W_\lambda(1118)$ (m \AA)	$W_\lambda(1128)$ (m \AA)	$W_\lambda(1305)$ (m \AA)
NiI	6635.12	4.42	−0.83	26	18	22	18
NiI	6643.63	1.68	−2.30	192	179	153	150
NiI	6767.77	1.83	−2.17	162	152	134	127
NiI	6772.31	3.66	−0.99	67	70	57	56
NiI	6842.04	3.66	−1.47	53	44	38	33
CuI	5105.54	1.39	−1.50	177	174	149	120
CuI	5782.12	1.64	−1.78	142	140	111	101
ZnI	4722.16	4.03	−0.39	...	39	56	63
ZnI	4810.54	4.08	−0.17	57	56	53	67
YII	4883.69	1.08	0.07	153	115	103	98
YII	5087.43	1.08	−0.17	84	71	72	78
YII	5200.42	0.99	−0.57	81
ZrI	6127.44	0.15	−1.06	102	75	32	16
ZrI	6134.55	0.00	−1.28	105	73	28	13
ZrI	6143.20	0.07	−1.10	104	78	37	16
BaII	5853.70	0.60	−1.01	167	160	140	132
BaII	6141.70	0.70	−0.07	242	234	199	193
BaII	6496.90	0.60	−0.38	238	224	198	193
LaII	6390.48	0.32	−1.41	75	65	48	30
LaII	6774.26	0.13	−1.72	83	66	53	30
NdII	5130.59	1.30	0.45	...	86	57	63
NdII	5319.81	0.55	−0.14	107	97	85	82
EuII	6645.11	1.38	0.12	72	62	46	56

Table 4. Derived Abundances for Pal 12

Star	S1			1118			1128			1305		
	[X/Fe]	σ^a	No.	[X/Fe]	σ^a	No.	[X/Fe]	σ^a	No.	[X/Fe]	σ^a	No.
Ion	(dex)	(dex)	Lines	(dex)	(dex)	Lines	(dex)	(dex)	Lines	(dex)	(dex)	Lines
OI	0.04	0.04	2	0.21	0.19	2	−0.06	0.21	2	0.07	0.13	2
NaI	−0.47	0.18	4	−0.52	0.16	4	−0.55	0.20	4	−0.49	0.16	4
MgI	−0.14	...	1	0.07	0.11	2	0.09	0.30	2	0.09	0.18	3
SiI	0.14	0.16	12	0.03	0.16	13	0.11	0.18	13	0.10	0.14	13
CaI	−0.17	0.24	13	−0.25	0.22	14	−0.18	0.19	14	−0.16	0.15	14
ScII	−0.16	0.17	6	−0.12	0.16	6	−0.08	0.16	7	−0.07	0.17	7
TiI	−0.10	0.21	26	−0.17	0.16	28	−0.12	0.25	33	−0.12	0.14	30
TiII	0.02	0.25	4	−0.03	0.13	5	0.08	0.18	6	0.08	0.10	5
VI	−0.31	0.19	8	−0.41	0.20	9	−0.35	0.15	10	−0.38	0.14	10
CrI	0.14	0.21	6	0.02	0.23	6	−0.03	0.20	10	0.07	0.21	10
MnI	−0.25	0.13	2	−0.28	0.09	2	−0.32	0.11	4	−0.28	0.20	5
FeI ^b	6.76	0.18	123	6.72	0.23	131	6.70	0.19	146	6.72	0.19	146
FeII	0.10	0.23	9	0.09	0.19	9	0.12	0.23	11	0.12	0.20	9
CoI	−0.35	0.21	4	−0.32	0.28	4	−0.29	0.21	4	−0.25	0.19	4
NiI	−0.11	0.17	21	−0.21	0.17	22	−0.20	0.19	23	−0.20	0.18	21
CuI	−0.55	0.18	2	0.14	0.16	2	−1.01	0.27	2	−0.69	0.07	2
ZnI	−0.45	...	1	−0.64	0.16	2	−0.51	0.18	2	−0.38	0.06	2
YII	−0.16	0.93	2	−0.60	0.52	2	−0.49	0.36	2	−0.35	0.17	3
ZrI	−0.16	0.07	3	−0.28	0.06	3	−0.22	0.05	3	−0.16	0.06	3
BaII	0.28	0.05	3	0.27	0.05	3	0.25	0.06	3	0.27	0.08	3
LaII	0.25	0.06	2	0.22	0.01	2	0.31	0.08	2	0.09	0.02	2
NdII	0.27	...	1	0.38	0.26	2	0.28	0.06	2	0.40	0.05	2
EuII	0.62	...	1	0.58	...	1	0.55	...	1	0.69	...	1

^aThis is the 1σ rms deviation of the set of abundances derived from each of the observed absorption lines about the mean abundance.

^bFor Fe I only, we give [Fe/H].

Table 5. Mean Abundances and Abundance Spreads for Four Stars in Pal 12

Species	Mean Abund. [X/Fe] (dex)	σ Around Mean (dex)	$\sigma(\text{Obs})$ (dex)	Spread Ratio ^a (dex)	No. of Stars ^b
OI	0.07	0.11	0.10	1.10	4
NaI	−0.51	0.04	0.09	0.42	4
MgI	0.08	0.01	0.10	0.11	3
SiI	0.10	0.05	0.05 ^c	0.90	4
CaI	−0.19	0.04	0.05	0.76	4
ScII	−0.11	0.04	0.07	0.62	4
TiI	−0.13	0.03	0.05 ^c	0.58	4
TiII	0.04	0.05	0.07	0.72	4
VI	−0.36	0.04	0.06	0.78	4
CrI	0.05	0.07	0.09	0.83	4
MnI	−0.28	0.03	0.09	0.30	4
FeI ^e	6.72	0.02	0.05 ^c	0.44	4
FeII	0.11	0.02	0.07	0.23	4
CoI	−0.30	0.04	0.11	0.39	4
NiI	−0.18	0.04	0.05 ^c	0.90	4
CuI	−0.52	0.49	0.12	4.05 ^d	4
ZnI	−0.51	0.13	0.07	1.86	3
YII	−0.48 ^f	0.12	0.19	0.67	3
ZrI	−0.20	0.06	0.05 ^c	1.12	4
BaII	0.27	0.01	0.05 ^c	0.24	4
LaII	0.22	0.09	0.05 ^c	1.80	4
NdII	0.35	0.07	0.07	1.06	3
EuII	0.61	0.06	4

^aThis is the ratio of σ about the mean abundance for Pal 12 of the sample of four stars to $\sigma(\text{Obs})$.

^bFor some species, Star S1, the coolest star in our Pal 12 sample, had significantly fewer usable lines, as the spectrum was more crowded and the lines became too strong to use.

^c $\sigma(\text{obs})$ is very low, in most cases due to the large number of lines used. It has been increased to 0.05 dex.

^dCu I has very large HFS corrections, between 0.5 and 1.0 dex.

^eFor Fe I only, we give [Fe/H].

^fThe coolest star is excluded; see §4.1.